

Why are there so few hot Jupiters?

W.K.M. Rice^{1*}, Philip J. Armitage^{2,3}, D.F. Hogg⁴

¹ *SUPA†, Institute for Astronomy, University of Edinburgh, Blackford Hill, Edinburgh, EH9 3HJ*

² *JILA, Campus Box 440, University of Colorado, Boulder CO 80309*

³ *Department of Astrophysical and Planetary Sciences, University of Colorado, Boulder CO 80309*

⁴ *School of Physics, University of Exeter, Stocker Road, Exeter, EX4 4QL*

2 February 2008

ABSTRACT

We use numerical simulations to model the migration of massive planets at small radii and compare the results with the known properties of ‘hot Jupiters’ (extrasolar planets with semi-major axes $a < 0.1$ AU). For planet masses $M_p \sin i > 0.5M_J$, the evidence for any ‘pile-up’ at small radii is weak (statistically insignificant), and although the mass function of hot Jupiters is deficient in high mass planets as compared to a reference sample located further out, the small sample size precludes definitive conclusions. We suggest that these properties are consistent with disc migration followed by entry into a magnetospheric cavity close to the star. Entry into the cavity results in a slowing of migration, accompanied by a growth in orbital eccentricity. For planet masses in excess of 1 Jupiter mass we find eccentricity growth timescales of a few $\times 10^5$ years, suggesting that these planets may often be rapidly destroyed. Eccentricity growth appears to be faster for more massive planets which may explain changes in the planetary mass function at small radii and may also predict a pile-up of lower mass planets, the sample of which is still incomplete.

Key words: solar system: formation — planets and satellites: formation — planetary systems: formation

1 INTRODUCTION

The first extrasolar planet discovered around a Solar-type star, 51 Pegasi b (Mayor & Queloz 1995), was the prototype of a class of exoplanets known as ‘hot Jupiters’. These are massive, gas giant planets, which for the purposes of this paper we define to orbit within 0.1 AU of their parent star. Although it has long been clear that the early discovery of 51 Peg was due to observational selection effects, and that the typical extrasolar planet orbits much further out (Marcy et al. 2005), hot Jupiters remain of particular interest for two reasons. First, the high temperatures of the protoplanetary disc at the radii where hot Jupiters now orbit (Bell et al. 1997) mean that it is extremely unlikely that these planets formed *in situ*. Rather, they must have formed at larger radii and then migrated inward to their current location. Although the same is probably also true of all extrasolar planets within the snow line (Garaud & Lin 2007), at larger radii the requirement for migration is a model-dependent statement whose validity rests on the accuracy of giant planet for-

mation models (Bodenheimer, Hubickyj & Lissauer 2000). Second, hot Jupiters orbit close enough that interactions with the star cannot be ignored. This makes them valuable testbeds for theories of tidal interaction (Ogilvie & Lin 2004; Ivanov & Papaloizou 2007) and planetary structure in the presence of irradiation (Burrows et al. 2007).

The best-developed model for the origin of hot Jupiters and other short-period planets attributes their migration to angular momentum loss to gas in the protoplanetary disc (Goldreich & Tremaine 1980; Lin & Papaloizou 1986). In this paper we consider primarily relatively massive planets, which are expected to migrate within gaps in the Type II regime¹. Observations provide two apparently contradictory constraints on such models. First, the radial distribution of planets is broadly consistent with that predicted by gas disc migration models (Armitage et al. 2002; Trilling, Lunine & Benz 2002; Ida & Lin 2004; Armitage 2007). This is true *even for the hot Jupiters*. In particular there is no substantial pile-up of planets at small radii that

¹ The lowest mass short-period planets — ‘hot Neptunes’ (Santos et al. 2004; McArthur et al. 2004) — may instead fall into the gap-less Type I regime (Ward 1997). Their origin poses different problems that we do not consider here.

* E-mail: wkmr@roe.ac.uk

† Scottish Universities Physics Alliance

would be indicative of an efficient mechanism stopping planets migrating into the star. Second though, the inner edge of the hot Jupiter distribution does not appear to coincide with the Roche limit, as might be expected if the current population of hot Jupiters is a remnant of a much bigger initial population that migrated inward on circular orbits. Rather, the inner edge for hot Jupiters occurs at a distance nearly twice that of the Roche limit, consistent with circularization from high eccentricity orbits in a planet-planet scattering model (Faber, Rasio & Willems 2005; Ford & Rasio 2006). To explain this within a disc migration model, we require a mechanism that depletes planets at radii beyond the Roche limit, but which does not slow migration so much as to yield far more hot Jupiters than are observed.

In this paper, we study the dynamical evolution of massive planets as they migrate into gas-poor magnetospheric cavities surrounding young stars. A large body of observational evidence suggests that the magnetic fields of T Tauri stars are typically strong enough to disrupt the inner regions of protoplanetary discs (Königl 1991; Bouvier et al. 2007), and the existence of this inner cavity will affect planet migration if the size of the cavity exceeds the stellar Roche limit. It is expected that the stellar magnetosphere will truncate the gas disc close to the co-rotation radius, where the Keplerian angular velocity of the disc is the same as the stellar angular velocity. Observationally, pre-main sequence stars have a bimodal distribution of rotation periods (Herbst et al. 2007), with one peak at periods of ~ 1 day and a second at periods of 5 – 8 days. Migration is expected to slow dramatically once planets pass inside the 2:1 resonance with the inner disc edge, so the existence of this long-period population appears consistent with hot Jupiters having orbital periods of 3 days or more (Lin, Bodenheimer & Richardson 1996). Indeed, given the prevalence of large magnetospheric cavities, the surprise is not that there are so many hot Jupiters, but rather *why are there so few?* In this paper, we argue that the answer lies in the fact that entry into the magnetosphere not only slows radial migration, but also excites orbital eccentricity. Since the rate of migration and the rate of eccentricity growth are directly linked (both are proportional to the gas surface density at the inner edge of the disc), planets entering the magnetosphere are destroyed as a consequence of eccentricity growth on a similar timescale to that on which they would accumulate at small radii. An inner edge to the hot Jupiter distribution is created without any substantial pile-up of planets there.

The plan of this paper is as follows. In Section 2 we describe our model for planet evolution within magnetospheric cavities. Results are presented in Section 3, and Section 4 summarizes our conclusions.

2 PLANET MIGRATION WITHIN STELLAR MAGNETOSPHERES

Accretion onto low-mass, pre-main sequence stars, known as T Tauri stars, is thought to occur via accretion along the stellar magnetic field lines. Since the accreting material is initially spiralling inwards through a circumstellar disc, the general idea (Ghosh & Lamb 1979) is that the disc will be truncated at the radius at which the ram pressure of the accreting material balances the magnetic pressure of the

stellar magnetic field. The material will then follow the field lines, giving rise to accretion streams and creating accretion shocks near the stellar magnetic poles. For accretion to occur, the truncation radius must be inside co-rotation, since outside co-rotation any material tied to the stellar magnetic field lines will gain angular momentum and will tend to move away from the star. At the late epochs relevant for studies of planet migration the accretion rate is low, so the most likely scenario is that the truncation radius is very close to the co-rotation radius. Stellar angular momentum considerations (Collier Cameron & Campbell 1993) also support the idea that the disc does not penetrate far inside corotation. Discs around T Tauri stars with rotation periods between 5 and 8 days would therefore be truncated at between 0.06 and 0.08 AU.

While the gas disc is still present, planets will migrate inwards via either Type I (Ward 1997) or Type II (Goldreich & Tremaine 1980) migration, depending on the mass of the migrating planet. Once inside co-rotation, and hence once inside the disc truncation radius, the planet migration should be quite different. Type I migration can no longer operate since there will be no mass at the locations of the nearby resonances to supply the differential Lindblad torques (Ward 1997). Type II will also not operate in the usual manner since the standard scenario is that disc viscosity causes material to flow into the gap, causing the gap and planet to move inwards on viscous timescales (Lin & Papaloizou 1986). Once the planet is inside co-rotation, however, the disc material flows along field aligned accretion streams, accreting onto the star near the magnetic poles, and does not flow into the gap. The low density gas within the magnetosphere does not materially affect the planet’s orbit (Papaloizou 2007). The planet can, however, interact gravitationally with the surrounding disc, and it is this process that we will investigate here.

2.1 Numerical simulations

We use the Zeus code (Stone & Norman 1992) to simulate the circumstellar gas disc. We work in two-dimensional cylindrical polar coordinates (r, ϕ) with a resolution of $n_r = 400$ and $n_\phi = 400$. The computational domain extends, in code units, from $r_{\text{in}} = 1$ to $r_{\text{out}} = 10$, and we impose outflow boundary conditions at both r_{in} and r_{out} . We assume the inner boundary is located at the corotation radius and so for a solar mass star with a rotation period of 8 days, the inner boundary is then located, in real units, at $r = 0.08$ AU. The use of an outflow boundary condition here then approximates the gas accretion onto the central star.

We assume that the disc is isothermal with a radially dependent sound speed given by $c_s(r) = 0.05r^{-1/2}$. The disc thickness h/r is related to the sound speed through $h/r \approx c_s/V_K$, giving a disc thickness of 0.05 at $r = 1$. We model angular momentum transport using a kinematic viscosity, ν , that operates only on the azimuthal component of the momentum equation (Papaloizou & Stanley 1986). The initial disc surface density, Σ , is taken to have a radial dependence of $\Sigma(r) \propto r^{-1}$. Since $\dot{M} \propto \nu \Sigma(r)$ and since we expect \dot{M} to be constant, we assume that $\nu(r) \propto r$ and normalise the viscosity using the standard alpha formalism, $\nu = \alpha c_s h$ (Shakura & Sunyaev 1973) with $\alpha = 10^{-3}$ at $r = 1$.

We adopt units in which $G = 1$ and the mass of the

star and planet satisfy $M_* + M_{\text{pl}} = 1$. We consider various planet masses and positions, but the planet is always located within $r = 1$, and the centre of mass is fixed at $r = 0$. The dynamics of the star and planet are integrated using a second-order scheme that is adequate for the relatively short durations (a few hundred planetary orbits) of our simulations. At the epoch of giant planet migration we would expect the surface density at ~ 0.1 AU to be $\sim 1000 \text{ g cm}^{-2}$ (Armitage & Clarke 1996). This would produce a physical migration timescale, for hot Jupiters, of $\sim 10^4$ years, corresponding to around 10^6 orbital periods at these small radii. We are able to evolve our simulations for only a few hundred orbital periods, and hence this surface density would not produce measurable changes in the planet's semi-major axis a or eccentricity e during the course of our simulations. To see evolution within a few hundred orbits we adopt a higher scaling for the surface density. This, however, does not affect the rate of eccentricity growth, measured as ade/da , because the accelerations in a and e are linear in disc mass (Armitage & Natarajan 2005; Artymowicz et al. 1991). We therefore use, in code units, $\Sigma = 0.01$ at $r = 1$. This corresponds, for a solar mass star with an 8 day rotation period, to a surface density of $1.4 \times 10^7 \text{ g cm}^{-2}$, a value $\sim 10^4$ times greater than what one would realistically expect, but which allows us to measure the rate of change of a and e in our simulations.

The simulations consider a star with mass M_* and planet with mass M_{pl} in orbit with semimajor axis a ($a < 1$) and initial eccentricity $e = 0.02$. The disc is initially azimuthally uniform and in Keplerian rotation about the centre of mass located at $r = 0$. In the presence of a planet, the disc surface density has a non-axisymmetric distribution that is approximately static in the corotating frame. At the start of the simulations, there is a transient phase as the disc adjusts from the axisymmetric initial conditions. These transients have no physical relevance, as real planet formation time scales are long compared to the orbital period. To avoid spurious migration in the transient phase, we evolve the simulations for 40 orbits at $r = 1$ without the disc mass being included in the calculation of the accelerations of the star and planet. After 40 orbits, the disc mass is turned on smoothly over 5 additional orbits.

3 RESULTS

The initial simulations considered planet masses of $M_{\text{pl}} = 0.001$ and $M_{\text{pl}} = 0.01$ and initial semimajor axes of $a_o = 0.9$, $a_o = 0.8$, $a_o = 0.7$, and $a_o = 0.6$. In all the simulations, the star's mass is set such that $M_* + M_{\text{pl}} = 1$. If we assume the central star has a mass of 1 solar mass, these two planets masses are roughly 1 and 10 Jupiter masses respectively. All of the simulations were evolved for at least 250 orbits at $r = 1$. As discussed above, during the first 40 orbits, the disc mass is not included in the star-planet orbit integration and is then turned on smoothly over the next 5 orbits.

Figure 1 shows the surface density structure of the disc just before including the backreaction of the disc on the star-planet orbit for $M_{\text{pl}} = 0.001$ (left hand panel) and $M_{\text{pl}} = 0.01$ (right hand panel). The centre of the images is located at the centre of mass of the star planet system and the images extend to $r = 5$. In both images the semimajor

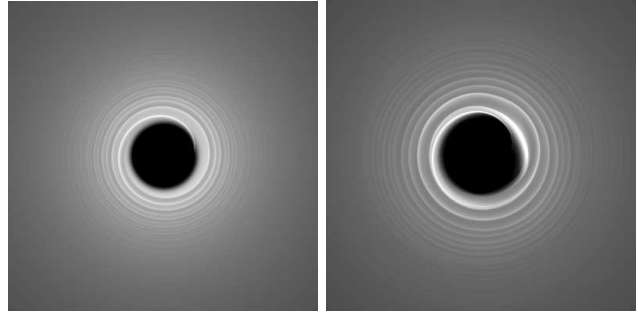


Figure 1. Disc surface density structure for $M_{\text{pl}} = 0.001$ (left hand panel) and $M_{\text{pl}} = 0.01$ (right hand panel) immediately prior to including the disc mass in the calculation of the star and planet accelerations. The centre of each image is located at the centre of mass of the star planet system, and the images extend to $r = 5$. In both images $a = 0.9$. Although the images are similar, the spiral density waves are stronger and extend further into the disc for $M_{\text{pl}} = 0.01$ than for $M_{\text{pl}} = 0.001$.

axis of the star-planet system is $a = 0.9$. Although similar, it is clear that the spiral arms are stronger and extend further into the disc for $M_{\text{pl}} = 0.01$ than for $M_{\text{pl}} = 0.001$.

3.1 $M_{\text{pl}} = 0.001$

The simulations all start with a small eccentricity ($e = 0.02$) and consider semimajor axes of $a_o = 0.9$, $a_o = 0.8$, $a_o = 0.7$, and $a_o = 0.6$. Figure 2 shows the semimajor axis evolution for $M_{\text{pl}} = 0.001$. Apart from the $a_o = 0.9$ case, the change in semimajor axis once the backreaction of the disc is included is very small, with absolutely no noticeable change for $a_o = 0.6$. The figure does show the planet starting at $a = 0.9$ migrating in to a smaller radius than the planet starting at $a = 0.8$. This is simply because when the planet starting at $a = 0.9$ reaches $a = 0.8$ it does not have exactly the same properties as the planet starting at $a = 0.8$, and therefore does not evolve in exactly the same way. Its migration does, however, slow considerably once inside $a = 0.8$, and its inward migration rate approaches a value similar to that of the planet starting at $a = 0.8$. The eccentricity is shown in Figure 3. Although we haven't labelled the individual curves, it is clear that apart from some sinusoidal variations, the mean eccentricity does not appear to vary significantly over the course of these simulations. These results suggest that planets of this mass will migrate rapidly inwards to $r \sim 0.8$ and then continue migrating more slowly, possibly becoming stranded at a radius of between $r = 0.7$ and $r = 0.6$.

We can also quantify the migration rate in these simulations. Assuming $r = 1$ corresponds to a real radius of 0.08 AU, our simulations are evolved for 4.6 years after the backreaction of the disc is included (i.e., from $t = 40$ orbits to $t = 250$ orbits with each orbit taking 8 days). The planet starting at $a_o = 0.9$ therefore actually starts at 0.072 AU and migrates inwards to 0.062 AU in 4.6 years. Our chosen surface density is, however, also about 10000 times greater than would be realistically expected. Since the migration rate depends linearly on the disc surface density (Armitage & Natarajan 2005; Artymowicz et al. 1991) a more realistic migration timescale in this case is 0.015 AU

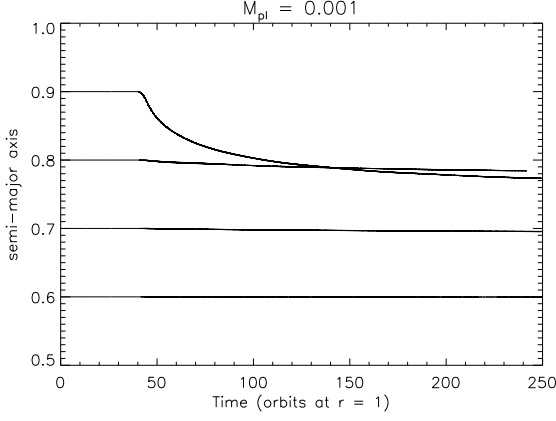


Figure 2. Semi major axis evolution for a planet mass of $M_{\text{pl}} = 0.001$ starting at $a_o = 0.9, 0.8, 0.7$, and 0.6 . The decay rate is quite substantial for $a_o = 0.9$, but decreases significantly with decreasing initial semi major axis. There is no noticeable inward migration for $a_o = 0.6$.

in 46000 years, giving a migration rate of $\dot{a} = 3.3 \times 10^{-7}$ AU/yr. Repeating this for $a_o = 0.8$ gives a migration rate of $\dot{a} = 2.8 \times 10^{-8}$ AU/yr. This is clearly small, but at this rate the planet could still move inwards by 0.01 AU in $\sim 3 \times 10^5$ years. For $a_o = 0.7$ and $a_o = 0.6$, the unscaled migration rates are $\dot{a} = 7 \times 10^{-9}$ AU/yr and $\dot{a} = 8 \times 10^{-10}$ AU/yr. Although a planet starting at $a_o = 0.7$ could migrate a further 0.01 AU in the disc lifetime (i.e., within a few million years), this is not possible for $a_o = 0.6$, requiring in excess of 10^7 years to do so.

In the above case, the angular momentum exchange between the planet and disc is likely to occur primarily through the 2:1 resonance. Figure 4 shows a representative, azimuthally averaged disc surface density profile just prior to the start of active integration. Although the inner edge of the disc is at $r = 1$, the peak of the surface density occurs at between $r = 1.2$ and $r = 1.3$. The 2:1 resonance with the peak of the surface density therefore occurs at between $r = 0.76$ and $r = 0.82$. The interpretation of the above result is that as the planet migrates inwards, the location of the 2:1 resonance moves inside the peak of the surface density, the angular momentum exchange becomes inefficient, and the migration stalls inside, but reasonably near, the radius that is in 2:1 resonance with the peak of surface density. This gives an orbital period for the planet that is close to half the rotation period of the central star.

3.2 $M_{\text{pl}} = 0.01$

We repeat the above simulations, keeping everything the same except the planet mass which is now $M_{\text{pl}} = 0.01$, 10 times more massive than that considered above and which corresponds, for our chosen scaling, to ~ 10 Jupiter masses. Figure 5 shows the semimajor axis evolution for $M_{\text{pl}} = 0.01$. This is considerably different to the $M_{\text{pl}} = 0.001$ case. All four cases show inward migration, with the rate being quite substantial for $a_o = 0.9$, $a_o = 0.8$, and $a_o = 0.7$. What is most interesting is that in the $a_o = 0.7$ case, the migration rate appears to accelerate after ~ 180 orbits. When we consider the eccentricity evolution, shown in Figure 6,

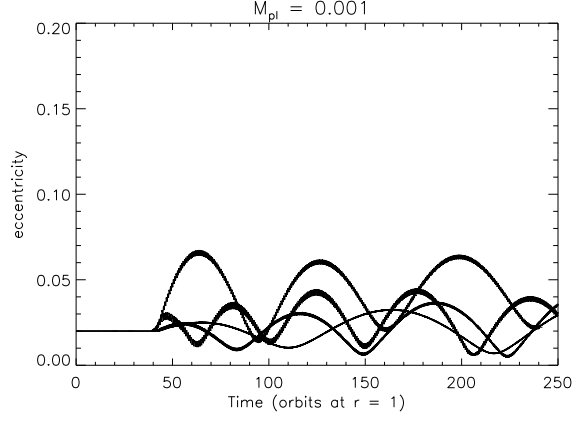


Figure 3. Eccentricity evolution for $M_{\text{pl}} = 0.001$ and for $a_o = 0.9, 0.8, 0.7$, and 0.6 . The eccentricity has been averaged over the orbital period to remove small scale fluctuations. Although there are some sinusoidal variations in the eccentricities, the mean eccentricity does not appear to change significantly in any of the 4 simulations.

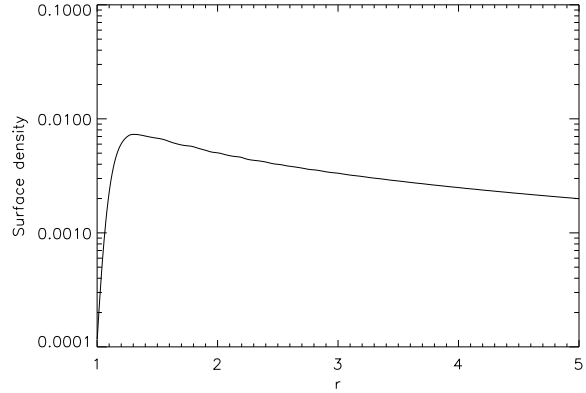


Figure 4. A representative, azimuthally averaged surface density profile, in this case from a simulation in which $M_{\text{pl}} = 0.001$ and $a_o = 0.9$. Although the disc inner edge is located at $r = 1$, the peak of the surface density occurs at between $r = 1.2$ and $r = 1.3$. A planet with mass $M_{\text{pl}} = 0.001$ appears to stall just inside the radius that is in 2:1 resonance with the peak of the surface density.

we see that in this case the eccentricity growth is substantial, increasing from $e = 0.02$ to $e = 0.27$ during the course of the simulation. There is still noticeable eccentricity growth for $a_o = 0.6$, but not much growth for $a_o = 0.9$ and $a_o = 0.8$ which are unlabelled in Figure 6. The angular momentum exchange between the planet and disc occurs generally through corotation resonances - which in the case of an eccentric planet may be non-coorbital - and Lindblad resonances. It is fairly well known that Lindblad resonances produce eccentricity growth, while corotation resonances produce eccentricity damping, and that if corotation resonances are present, they will tend to dominate (Goldreich & Tremaine 1980). A way in which eccentricity growth can occur, however, is if the gap around a planet is large enough that the outer resonance still operates, but the corotation resonances do not (D'Angelo, Lubow & Bate 2006; Artymowicz et al. 1991). Our simulations, therefore,

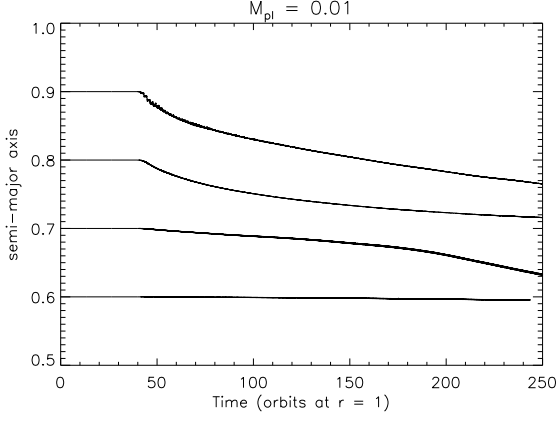


Figure 5. Semi major axis evolution for a planet mass of $M_{\text{pl}} = 0.01$ starting at $a_o = 0.9, 0.8, 0.7$, and 0.6 . The decay rate is quite substantial for all initial semi major axes except $a_o = 0.6$, which still has non-negligible inward migration. What is most interesting is how, for $a_o = 0.7$, the inward migration appears to accelerate after about 180 orbits.

suggest that when the planet is at large radii ($a = 0.9$, and $a = 0.8$) the outer Lindblad resonances do not dominate sufficiently to produce significant eccentricity growth. At smaller radii ($a = 0.7$), however, the gap is effectively larger, the inner resonances no longer operate efficiently, and the outer resonances, primarily the 1:3 resonance (D’Angelo, Lubow & Bate 2006; Artymowicz et al. 1991), act to produce eccentricity growth. As the planet moves to even smaller radii ($a = 0.6$), the outer resonances stop operating efficiently, and the eccentricity growth rate starts to decrease.

These simulations suggest that the more massive planet will migrate inwards rapidly until reaching $a \approx 0.7$ at which radius it will start to undergo rapid eccentricity growth. Unlike the lower mass case, there is no evidence here that the planet migration is likely to stall and we see inward migration and eccentricity growth even for the smallest initial semimajor axis considered. Figure 7 shows the long term evolution in semimajor axis and eccentricity for a $M_{\text{pl}} = 0.01$ planet starting at $a = 0.9$. The figure shows that the initially the eccentricity growth is small but that the rate of eccentricity growth increases rapidly when $a \sim 0.7$. As the planet continues migrating inwards the eccentricity growth rate does decrease, but at the end of the simulation the planet is still migrating inwards and its eccentricity is still increasing. If we again assume our inner disc radius corresponds to a real radius of 0.08 AU, at the end of this simulation the planet will have a periastron distance of only 5.5 solar radii. The simulation is evolved for 1000 orbits at $r = 1$ which, if we assume a radial scaling of 0.08 AU, corresponds to a time of about 4000 days. As discussed earlier, our chosen surface density is about 10000 times greater than a realistic surface density. A more realistic timescale for this evolution is therefore $\sim 10^5$ years, which is well within the disc lifetime. Since young stellar objects generally have radii of a few solar radii, and since this planet is still migrating inwards at the end of this long simulation, it seems quite likely that it will ultimately collide with the central star.

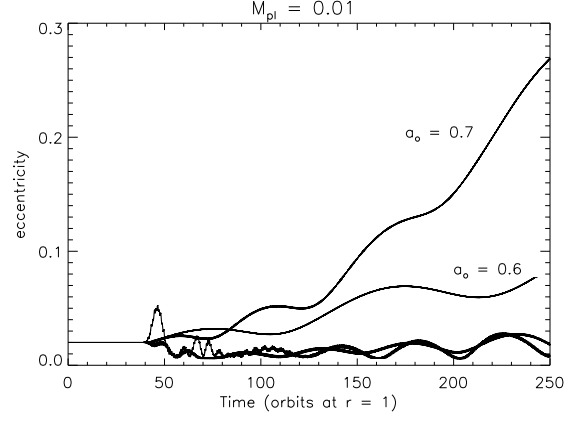


Figure 6. Eccentricity evolution for $M_{\text{pl}} = 0.01$ and for $a_o = 0.9, 0.8, 0.7$, and 0.6 . The eccentricity has been averaged over the orbital period to remove small scale fluctuations. What is evident from the figure is that a planet starting at $a_o = 0.7$ or $a_o = 0.6$ will undergo substantial eccentricity growth, in particular for $a_o = 0.7$ in which the eccentricity grows from $e = 0.02$ to $e = 0.27$ during the simulation.

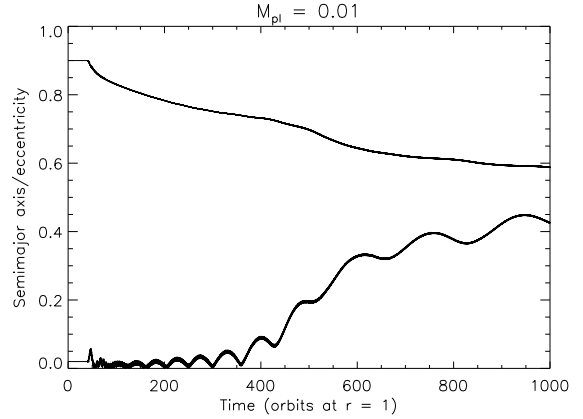


Figure 7. Semimajor axis (upper curve) and eccentricity (lower curve) evolution for a $M_{\text{pl}} = 0.01$ planet starting at $a = 0.9$, and evolved for 1000 orbits. It is clear that when this planet reaches $a \sim 0.7$, it undergoes rapid eccentricity growth, the rate of which decreases as it moves further inwards, but at the end of the simulation is still not negligible.

3.3 $a_o = 0.7$

To further investigate how eccentricity growth varies with planet mass, we have considered additional planet masses of $M_{\text{pl}} = 0.005$, and $M_{\text{pl}} = 0.0005$, corresponding for our chosen scaling, to roughly 5, and 0.5 Jupiter mass planets, both with initial semimajor axes of $a_o = 0.7$. This initial semimajor axis is chosen because it showed the greatest eccentricity growth in the $M_{\text{pl}} = 0.01$ simulations.

Figure 8 shows the eccentricity growth for all the simulations starting with $a_o = 0.7$. The $M_{\text{pl}} = 0.01$ and $M_{\text{pl}} = 0.005$ cases are labelled, while the eccentricity evolution for the other 2 planet masses ($M_{\text{pl}} = 0.001$ and $M_{\text{pl}} = 0.0005$) are very similar and can’t be easily distinguished. What is clear is that the eccentricity growth rate decreases with decreasing mass. Fitting straight lines to the

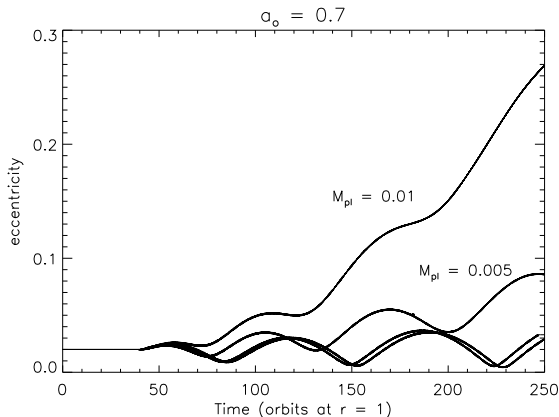


Figure 8. Eccentricity growth for planet masses of $M_{\text{pl}} = 0.01$, $M_{\text{pl}} = 0.005$, $M_{\text{pl}} = 0.001$, and $M_{\text{pl}} = 0.0005$ all starting at $a_o = 0.7$. For our chosen scaling these correspond to planet mass of 10, 5, 1, and 0.5 Jupiter masses. What is clear is that the eccentricity growth rate decreases with decreasing planet mass. For realistic surface densities and assuming an inner disc radius at 0.08 AU, the two most massive planets can undergo substantial eccentricity growth in a time of $\sim 10^5$ years.

eccentricity curves between $t = 40$ orbits and $t = 250$ orbits we find, for our chosen scaling, eccentricity growth rates, in order of decreasing planet mass, of $\dot{e} = 4.8 \times 10^{-6} \text{ yr}^{-1}$, $\dot{e} = 1.3 \times 10^{-6} \text{ yr}^{-1}$, $\dot{e} = 1.0 \times 10^{-7} \text{ yr}^{-1}$, and $\dot{e} = 3.1 \times 10^{-8} \text{ yr}^{-1}$. The latter two growth rates should be treated somewhat cautiously since the error in these values will be large compared to the values themselves. These growth rates do, however, suggest that planets with masses greater than 1 Jupiter mass may undergo substantial eccentricity growth in a time of $\sim 10^5$ years, while lower mass planets may require 10^6 years or longer. This is at least consistent with the lack of a pile-up of hot Jupiters at small radii, but may predict a pile-up of lower mass planets, the sample of which today is still incomplete.

It should however be noted that eccentricity growth rates appear to depend on the disc viscosity (D’Angelo, Lubow & Bate 2006; Kley & Dirksen 2006). Eccentricity growth can be sustained in discs with α less than a few times 10^{-3} and increases with decreasing α , while α values in excess of 10^{-2} may ultimately damp eccentricity growth (D’Angelo, Lubow & Bate 2006). Moorhead & Adams (2007) similarly argue that eccentricity growth depends strongly on the properties of the gap, which is determined both by the disc viscosity and the planet mass (Syer & Clarke 1995). Our simulations involve analogous, but not identical considerations. In our case viscosity is unimportant within the cavity (by assumption in the simulations, and also physically), and the gap edge is set by the balance between viscosity and magnetospheric, rather than gravitational, torques.

4 DISCUSSION AND CONCLUSION

In this paper we have considered star-planet systems with initially small eccentricities and with orbital radii $a < 1$, surrounded by a circumstellar disc extending from $r = 1$ to

$r = 10$. The inner edge of the disc is assumed to be truncated by the stellar magnetic field close to corotation and we assume that the planet has migrated inwards through the disc and is now inside the magnetospheric cavity. We have generally assumed that the inner edge of our disc corresponds to a real radius of 0.08 AU, as expected for a stellar rotation period of 8 days.

Our initial simulations consider planet masses of $M_{\text{pl}} = 0.001$ and $M_{\text{pl}} = 0.01$ and initial semimajor axes of $a_o = 0.9$, $a_o = 0.8$, $a_o = 0.7$, and $a_o = 0.6$. The $M_{\text{pl}} = 0.001$ simulation, which is taken to represent a ~ 1 Jupiter mass planet, initially migrates inwards rapidly, but appears to stall at a radius of between $r = 0.6$ and $r = 0.7$. This is close to the radius that is in 2:1 resonance with the peak of the disc surface density which in our simulations is just outside the inner edge of the disc. Assuming a stellar rotation period of 8 days, this suggests that these planets would stall with orbital periods of ~ 4 days. More generally, the planet would stall with an orbital period a little less than half the stellar rotation period.

The $M_{\text{pl}} = 0.01$ simulation was significantly different. The inward migration was much more rapid and the simulation starting with $a_o = 0.7$ showed significant eccentricity growth. To produce observable changes within the few hundred orbits of our simulations, we used surface densities significantly higher than would be realistically expected. After scaling the surface density to a more reasonable value, this planet would survive $\sim 10^5$ years before colliding with the central star. To further investigate this process we repeated this simulation ($a_o = 0.7$) but varied the planet mass from $M_{\text{pl}} = 0.01$ down to $M_{\text{pl}} = 0.0005$. As expected, the eccentricity growth rate increased with increasing planet mass, with the lowest mass planet showing very little or no eccentricity growth, while the eccentricity of the most massive planet increased substantially. The growth rates calculated assuming stellar rotation periods of 8 days, and reasonable disc surface densities, suggest that planets with masses in excess of 1 Jupiter mass could undergo substantial eccentricity growth in $\sim 10^5$ years, while the lower mass planets need 10^6 years or longer. The exact mass range for which we might expect substantial eccentricity growth is, however, difficult to accurately quantify as it depends not only on the disc surface density, but also on the disc viscosity (D’Angelo, Lubow & Bate 2006).

These general results of our simulations appear at least qualitatively consistent with current observational evidence. That eccentricity growth rates increase with increasing mass is consistent with the possible deficit of massive planets at small radii (Zucker & Mazeh 2002) and is also at least qualitatively consistent with the lack of any significant pile-up of giant planets at small radii. These simulations also suggest that some planets could be left stranded on eccentric orbits if the disc dissipates prior to these planets colliding with the central star. The decrease in migration rate with decreasing mass would imply that there should be some mass range for which this becomes quite likely, i.e., when the eccentricity growth timescale approaches the disc lifetime. Ford & Rasio (2006) suggest that if hot Jupiters migrate inwards on orbits with reasonably small eccentricities and then become tidally locked to the central star, the inner edge of the hot Jupiter population should be close to the Roche limit, the distance at which a planet fills its Roche lobe. They find, however,

that the inner edge of the hot Jupiter population appears to be located at twice the Roche limit, rather than at the Roche limit itself, as would occur if these planets are tidally circularised from highly eccentric orbits (Faber, Rasio & Willems 2005).

What is also interesting is that this does not appear to be true for the lowest mass close-in planets observed to date, the “hot Neptunes”, a few of which appear to exist close to their Roche limit. This is again qualitatively consistent with our result that the lowest mass planets undergo very little eccentricity growth. The inner edge of this population should then occur at the Roche limit, rather than at twice the Roche limit as would occur if they were tidally circularized from an eccentric orbit. This result would also suggest that we might expect a pile-up of low-mass close-in planets, as their inward migration appears to stall with a period a little less than half the stellar rotation period.

Since the eccentricity growth rate depends on both the disc mass and viscosity, it is difficult to quantify the exact mass at which we would expect eccentricity growth to become negligible. However, our simulation results do suggest three primary outcomes:

- Low-mass planets migrate inwards on roughly circular orbits and will stall with an orbital period close to half the rotation period of the central star. The inner edge of this population should be located near the Roche limit. Since these planets do not migrate into the central star, we would predict a pile-up of low-mass planets at small radii.
- High-mass planets undergo significant eccentricity growth and should collide with the central star - for reasonable disc viscosities and masses - in a time of $\sim 10^5$ years.
- Intermediate-mass planets, and some high-mass planets, could be stranded on eccentric orbits if the disc dissipates sufficiently quickly. These would then be tidally circularized and the inner edge of this population would be located at twice the Roche limit (Ford & Rasio 2006).

ACKNOWLEDGEMENTS

This work was supported by NASA’s ATP program under grants NNG04GL01G and NNX07AH08G, and by the NSF under grant AST 0407040.

REFERENCES

- Armitage, P. J. 2007, *ApJ*, 665, 1381
- Armitage, P.J., & Clarke, C.J. 1996, *MNRAS*, 280, 458
- Armitage, P. J., Livio, M., Lubow, S. H., & Pringle, J. E. 2002, *MNRAS*, 334, 248
- Armitage, P.J., & Natarajan, P. 2005, *ApJ*, 634, 921
- Artymowicz, P., Clarke, C.J., Lubow, S.H., & Pringle, J.E. 1991, *ApJ*, 370, L35
- Bell, K. R., Cassen, P. M., Klahr, H. H., & Henning, Th. 1997, *ApJ*, 486, 372
- Bodenheimer, P., Hubickyj, O., & Lissauer, J. J. 2000, *Icarus*, 143, 2
- Bouvier, J., Alencar, S.H.P., Harries, T.J., Johns-Krull, C.M., & Romanova, M.M. 2007, in *Protostars and Planets V*, ed. B. Reipurth, D. Jewitt, & K. Keil (Tucson: Univ. Arizona Press), 479
- Burrows, A., Hubeny, I., Budaj, J., & Hubbard, W. B. 2007, *ApJ*, 661, 502
- Butler, R. P., et al. 2006, *ApJ*, 646, 505
- Collier Cameron, A.C., & Campbell, C.G. 1993, *A&A*, 274, 309
- Cumming, A. 2004, *MNRAS*, 354, 1165
- D’Angelo, G., Lubow, S.H., & Bate, M.R. 2006, *ApJ*, 652, 1698
- Faber, J.A., Rasio, F.A., & Willems, B. 2005, *Icarus*, 175, 248
- Fischer, D. A., & Valenti, J. 2005, *ApJ*, 622, 1102
- Ford, E.B., & Rasio, F.A. 2006, *ApJ*, 638, L45
- Garaud, P., & Lin, D. N. C. 2007, *ApJ*, 654, 606
- Ghosh, P., & Lamb, F.K. 1979, *ApJ*, 232, 259
- Goldreich, P., & Tremaine, S. 1980, *ApJ*, 241, 425
- Herbst, W., Eisloffel, J., Mundt, R., & Scholz, A. 2007, in *Protostars and Planets V*, ed. B. Reipurth, D. Jewitt, & K. Keil (Tucson: Univ. Arizona Press), 297
- Ida, S., & Lin, D.N.C. 2004, *ApJ*, 616, 567
- Ivanov, P. B., & Papaloizou, J. C. B. 2007, *MNRAS*, 376, 682
- Kley, W., & Dirksen, G. 2006, *A&A*, 447, 369
- Königl, A. 1991, *ApJ*, 370, L39
- Lin, D. N. C., & Papaloizou, J. 1986, *ApJ*, 307, 395
- Lin, D.N.C., Bodenheimer, P., & Richardson, D.C. 1996, *Nature*, 380, 606
- Marcy, G., Butler, R. P., Fischer, D., Vogt, S., Wright, J. T., Tinney, C. G., & Jones, H. R. A. 2005, *Prog. Theor. Phys. Supp.*, 158, 24
- Mayor, M., & Queloz, D. 1995, *Nature*, 378, 35
- McArthur, B.E., et al. 2004, *ApJ*, 614, L81
- Moorhead, A.V., & Adams, F.C. 2007, *Icarus*, in press
- Ogilvie, G. I., & Lin, D. N. C. 2004, *ApJ*, 610, 477
- Papaloizou, J.C.B. 2007, *A&A*, 463, 775
- Papaloizou, J.C.B., & Stanley, G.Q.G. 1986, *MNRAS*, 220, 593
- Santos, N.C., et al. 2004, *A&A*, 426, L19
- Shakura, N.I., & Sunyaev, R.A. 1973, *A&A*, 24, 337
- Stone, J.M., & Norman, M.L. 1992, *ApJS*, 80, 753
- Syer, D., & Clarke, C.J. 1995, *MNRAS*, 277, 758
- Tabachnik, S., & Tremaine, S. 2002, *MNRAS*, 335, 151
- Trilling, D. E., Lunine, J. I., & Benz, W. 2002, *A&A*, 394, 241
- Ward, W.R. 1997, *Icarus*, 126, 261
- Zucker, S., & Mazeh, T. 2002, *ApJ*, 568, L113